Chemical Science

Chemical Science

Edge Article

Turning on the Biradical State of Tetracyano- Perylene and Quaterrylenequinodimethanes by Incorporation of Additional Thiophene Rings

Zebing Zeng,[a] Sangsu Lee,[b] José L. Zafra,[c] Masatoshi Ishida,[b] Nina Bao,[d] Richard D. Webster,[e] Juan T. López Navarrete,*[c] Jun Ding,*[d] Juan Casado,*[c] Dongho Kim,*[b] and Jishan Wu*[af]

Polycyclic hydrocarbon with a singlet biradical ground state has recently become a hot topic among various studies on π-conjugated systems and it is of importance to understand the fundamental *structure-biradical character-physical properties* relationship. In this work, we found that after incorporation of two additional thiophene rings to the closed-shell tetracyano- perylene (**Per-CN**) and quaterrylenequinodimethanes (**QR-CN**), the obtained new quinoidal compounds **QDTP** and **QDTQ** became a singlet biradical in the ground state due to the recovery of aromaticity of the thiophene rings in the biradical form and additional steric repulsion between the thiophene rings and the rylene unit. The ground state geometries and electronic structures of **QDTP** and **QDTQ** were systematically studied by variable-temperature nuclear magnetic resonance, electron spin resonance, superconducting quantum interference device and FT Raman spectroscopy, assisted by density functional theory calculations. Both compounds were found to be a singlet biradical in the ground state with a small singlet-triplet energy gap and the biradical character was enlarged by elongation of the π-conjugation length. Strong one-photon absorption and large two-photon absorption cross-sections were observed for both compounds in near-infrared region. Our studies demonstrated that a slight structural modification could significantly change the ground state and the electronic, optical and magnetic properties of a pro-aromatic π-conjugated system, and finally lead to new materials with unique properties.

Introduction

Recently, polycyclic hydrocarbons (PHs) with a singlet biradical ground state[1] have attracted much attention due to their unique optical, electronic and magnetic properties and promising applications for non-linear optics,[2] molecular electronics,[3] organic photovoltaics,[4] organic spintronics[5] and energy storage devices.[6] A fundamental reason for the appearance of a singlet biradical ground state can be ascribed to the gain of additional aromatic sextet rings in the biradical form in comparison to the closed-shell form. Good examples are Kubo's teranthene and quarteranthene molecules in which three and four additional aromatic sextet rings are obtained in the respective biradical forms, which can compensate the energy required to break an sp^2-sp^2 double bond.[7] Other examples are quinoidal hydrocarbons including indenofluorenes,[8] bis(phenalenyls)[9] and zethrenes,[10] in which a pro-aromatic quinodimethane unit such as *p*-quinoidimethane (*p*-QDM), 2,6-naphthoquinodimethane and 2,6-anthraquinodimethane is embedded into an aromatic framework. In addition, extended *p*-QDMs[11] and their thiophene analogs[12] with chain-length dependent ground states were recently reported. For example, our group has synthesized a series of tetracyano-oligo(*N*-annulated perylene (NP))quinodimethanes (**Per-CN** and **nPer-CN**, n = 2-6, Fig. 1).[11a] It was found that the monomer **Per-CN** has a closed-shell ground state while all of the higher oligomers **nPer-CN**s have a biradical ground state, and the steric repulsion between the NP units serves as the major driving force to rupture the quinoidal structure into a biradical configuration. When the two NP units in **2Per-C**N are fused together, the obtained tetracyano- quaterrylenequinodimethane **QR-CN** (Fig. 1)

becomes a closed-shell quinoid in the ground state due to the efficient double spin polarization through a planarized quaterrylene framework.[11b]
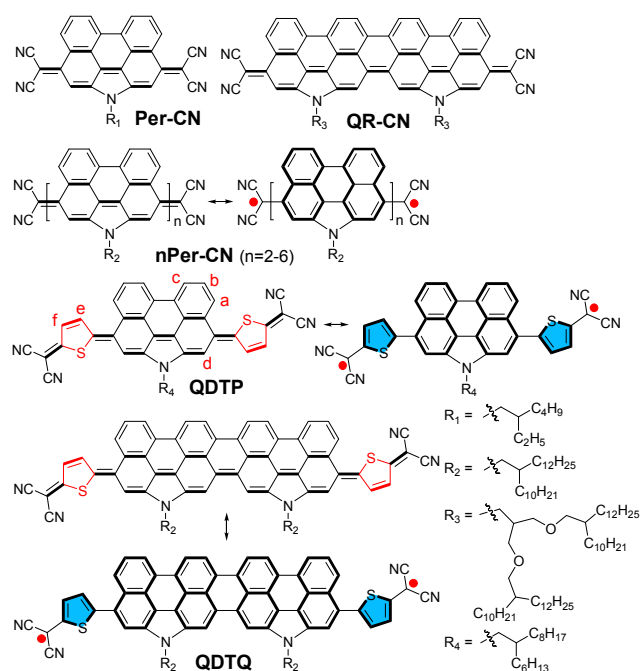

Fig. 1 Chemical and resonance structures of **Per-CN**, **nPer-CN**s, **QR-CN**, **QDTP** and **QDTQ**.

In principle, the closed-shell **Per-CN** and **QR-CN** can be also drawn in an open-shell biradical form similar to **nPer-CN**s, and then the particular questions arise: (1) how to turn on their biradical state, and (2) what are the differences between their physical properties under different ground states? Answers to these questions will help us to understand the fundamental *structure-biradical character-physical properties* relationship and thereby enable a tailored design. We expected that incorporation of a thiophene ring between the dicyanomethane moiety and the NP unit may significantly increase the biradical character of the molecules due to the recovery of the aromaticity of the quinoidal thiophene in the biradical form (Fig. 1). Thiophene ring was chosen rather than benzene ring due to the synthetic feasibility for the former (*vide infra*). To validate this assumption, quinoidal perylene **QDTP** and quaterrylene **QDTQ** containing two thiophene units were designed and synthesized (Fig. 1). Their geometries and electronic structures in the ground state were systematically investigated by variable-temperature nuclear magnetic resonance (VT-NMR), electron spin resonance (ESR), superconducting quantum interference device (SQUID) measurements and FT Raman spectroscopy, assisted by density functional theory (DFT) calculations. Their physical properties were studied by steady-state and transient absorption (TA) spectroscopy, two-photon absorption (TPA) and cyclic voltammetry. Our studies revealed that both **QDTP** and **QDTQ** showed a singlet biradical ground state with very different physical properties from those of **Per-CN** and **QR-CN**.

Results and discussion

Synthesis

As shown in Scheme 1, the target compounds **QDTP** and **QDTQ** were prepared by Takahashi coupling[13] from the corresponding dibromo- dithienoperylene **3** and dibromo- dithienoquaterrylene **7**, followed by oxidative dehydrogenation. Firstly, two thiophene units were attached to the active *peri*-position of NP by a two-fold Stille coupling reaction between the dibromo- NP **1** and tributyl-(thiophen-2-yl) stannane to give the dithienoperylene **2** in 75% yield (Scheme 1). Compared to the simple monomer **Per-CN**, longer branched aliphatic chain (R₄, 2-hexyldecyl) was introduced to surmount the solubility problem for the subsequent synthetic steps. Bromination of compound **2** with two equiv *N*-bromosuccinimide (NBS) afforded the key intermediate **3** in 87%

yield. Takahashi coupling reaction of **3** with malononitrile gave the crude precursor, which was partially dehydrogenated in the air. Subsequent oxidation of the crude product by a catalytic amount of *p*-chloranil in acetonitrile resulted in immediate precipitation of the target compound **QDTP** from the mixture, which was further carefully purified by silica gel column chromatography.

The synthesis of the more extended dithienoquaterrylenequinodimethane **QDTQ** is challenging because a fused quaterrylene framework has to be built up first. Our previous attempts to conduct direct intramolecular oxidative cyclodehydrogenation of the dibromo- NP dimer **4** carrying two 2-decyltetradecyl substituents (R₂ in Figure 1) gave an insoluble mixture due to the strong π-π stacking of the obtained quaterrylene molecules, which hampered the subsequent coupling reactions.[11b] Therefore, a highly branched alkyl ether group (R₃, Fig. 1) has to be used. In this study, we fortunately found that the dibromo- dithieno- NP dimer **6** with the 2-decyltetradecyl chains can be successfully cyclodehydrogenated by using 2,3-dichloro-5,6-dicyano-1,4-benzoquinone (DDQ) and Sc(OTf)₃ and afforded the key intermediate **7**, which is soluble in common organic solvents and possesses an absorption spectrum similar to the previously reported bis-*N*-annulated quaterrylene[14] (Fig. S1 in the Electronic Supplementary Information (ESI)†). The good solubility of **7** can be explained by the existence of large torsional angle between the thiophene ring and the quaterrylene unit which partially suppresses the π-π stacking and thus there is no need to introduce the synthetically demanding R₃ substituents. The intermediate **6** was prepared by a similar Stille coupling-followed-by-bromination sequence starting from the dibromo-NP dimer **4**.[11a] Compound **7** was then converted into the target compound **QDTQ** by similar Takahashi coupling followed by spontaneous oxidation in air without the need to use additional oxidants such as *p*-chloranil. Both **QDTP** and **QDTQ** are soluble in common solvents such as chloroform, toluene and THF. These deeply coloured products are stable in both solid state and in solution, except that **QDTQ** partially decomposed on a silica gel column, which prevented us from separating even longer homologs. The high-resolution mass spectra (MALDI-TOF) agreed well with their corresponding molecular weight, and the purity of the final products was further confirmed by high performance liquid chromatography and elemental analysis (see ESI†).
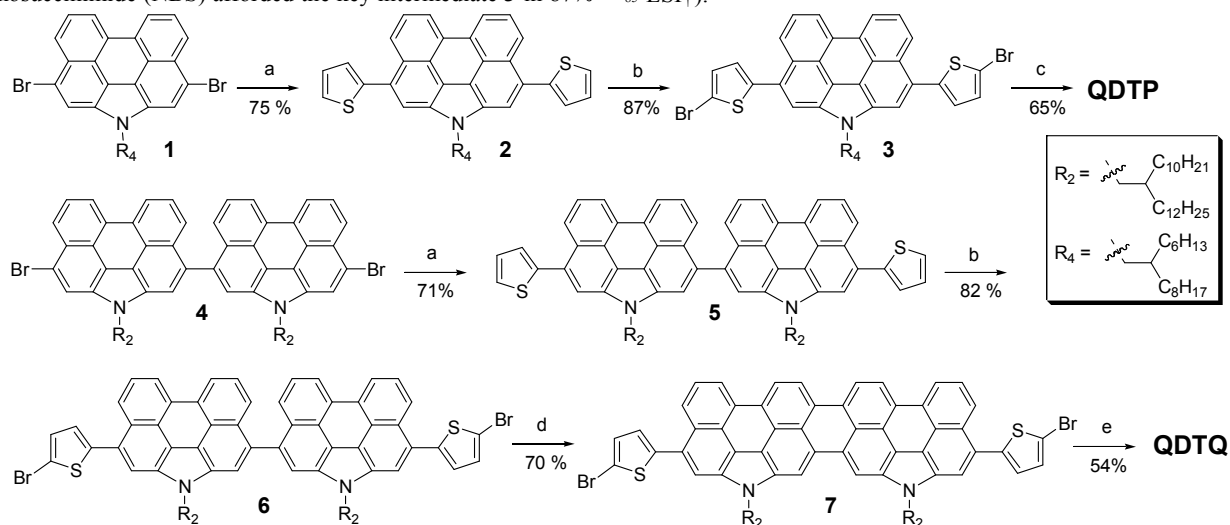
Scheme 1. Synthesis of **QDTP** and **QDTQ**. *Reagents and conditions*: (a) tributyl-(thiophen-2-yl)stannane, Ph(PPh₃)₄, toluene/DMF, 80 °C, 24 h; (b) NBS (2 equiv), DCM/DMF, 0 °C - 25 °C, 4 h; (c) (i) malononitrile, NaH, Pd(PPh₃)₂Cl₂, reflux, 48 h; (ii) HCl (2M); (iii) *p*-chloranil, CH₃CN, r.t.; (d) DDQ, Sc(OTf)₃, toluene, reflux, 24 h; (e) (i) malononitrile, NaH, Pd(PPh₃)₂Cl₂, reflux, 60 h; (ii) HCl (2M), air.
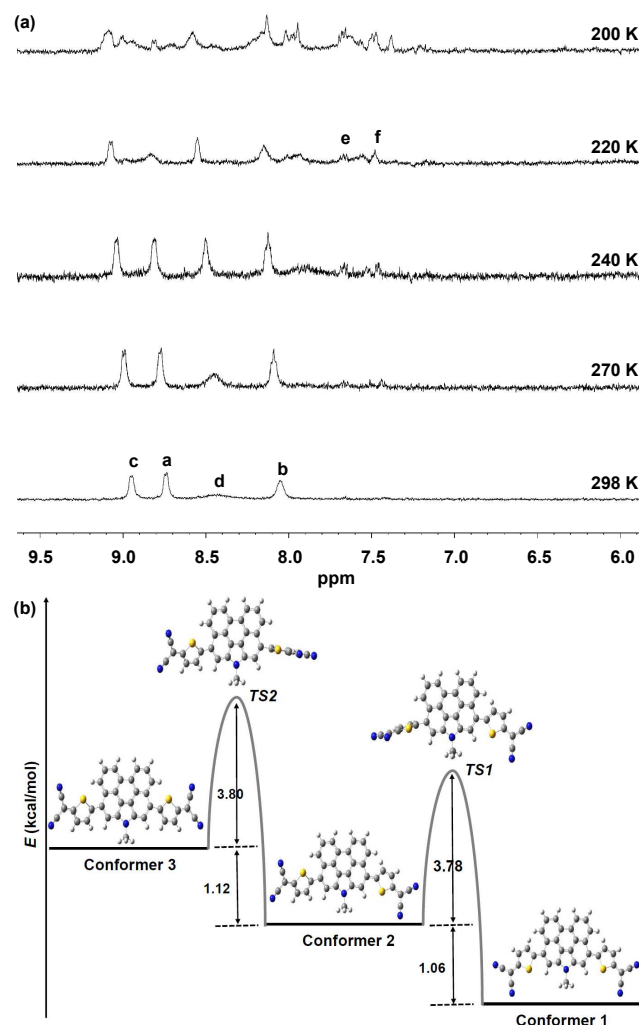
Edge Article

Magnetic properties

Fig. 2 (a) Variable temperature ^{1}H NMR spectra (aromatic region) of
5 **QDTP** in THF-d_8. The resonance assignment referred to the structure
shown in Figure 1. (b) Energy diagram of three conformers of **QDTP** and
their inter-conversion transition states.

ESR measurements of the solids of both **QDTP** and **QDTQ**
displayed intense one-line signals at g_e = 2.0030 and the intensity
10 decreases when the temperature is lowered (Fig. S2 in ESI†).
While **QDTQ** in various solvents showed strong ESR signals, a
solution of **QDTP** only exhibited a weak ESR signal under the
same condition probably due to smaller spin concentration. The
VT ^{1}H NMR spectra of **QDTP** recorded in THF-d_8 are shown in
15 Fig. 2a. Sharp resonance signals well-assigned to proton "a", "b"
and "c" of the central NP unit were observed upon cooling from
298 to 220 K. In contrast, the resonance for proton "d" showed
obvious changes with temperature, which was significantly
broadened at 298 K but became sharper as the temperature
20 decreased. Nevertheless, no clear peaks were detected for protons
"e" and "f" on the thiophene rings at room temperature but the
resonances appeared at low temperatures. These findings indicate

that **QDTP** exists as a singlet biradical in the ground state, which
is in equilibrium with a thermally excited triplet biradical. From
25 a view point of molecular structures, the quinoidal **QDTP** may
exist as three conformers with different configurations through
the ethylene linkage (Fig. 2b). DFT calculations predicted a small
energy difference (ca. 1 kcal/mol) between the different
conformers and the energy barrier from the highest-energy
30 conformer 3 to the middle-energy conformer 2 and then to the
lowest-energy conformer 1 is also small (ca. 3.8 kcal/mol) (Fig.
2b), which allow a fast inter-conversion between different
conformers at the room temperature. The large biradical character
may weaken the double bond character between the thiophenes
35 and the rylene unit and lead to a small rotation energy barrier. In
fact, calculations also predicted that the bond length between the
thiophene rings and the rylene unit is 1.43 Å (see ESI) in the
ground state, indicating a large single bond character. Such a
small energy barrier isomerization process can explain the
40 observed complicated NMR spectra at low temperatures (e.g.,
200 K), that is to say, inter-conversion is slower than the NMR
time scale when the temperature is below a certain point. On the
other hand, compound **QDTQ** showed NMR silence even at very
low temperature (-100 ^{o}C in CD_2Cl_2), indicating that this
45 extended derivative has a larger biradical character and a very
small singlet-triplet energy gap (ΔE_{S-T}), resulting in a large
population of triplet species.
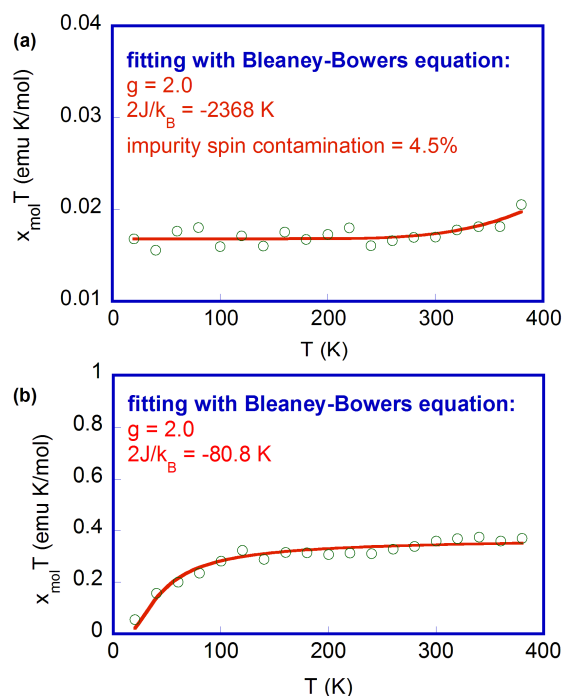
Fig.3 χ T-T curves in the SQUID measurements for the powder of (a)
50 **QDTP** and (b) **QDTQ**. The solid lines are the fitting curves according to
Bleaney-Bowers equation; g-factor was taken to be 2.

SQUID measurements were conducted for the powders of
QDTP and **QDTQ** at 5–380 K and the temperature dependent
magnetic signal changes indicated that both compounds have a
55 singlet biradical ground state (Fig. 3). The singlet-triplet energy

gap ΔE_{S-T} (i.e., $2J/k_B$) were estimated to be -4.71 kcal/mol (-2368 K) for **QDTP** and -0.16 kcal/mol (-80.8 K) for **QDTQ** by careful fitting of the data with Bleaney-Bowers equation.[15] The small singlet-triplet gaps allow facile thermal excitation to the higher
5 energy triplet biradical state and lead to NMR signal broadening. In particular, the **QDTQ** has a very small singlet-triplet gap and the triplet biradical species become dominant at room temperature and thus it is NMR silent.

Raman characterizations

10 Raman spectroscopy is a unique tool to evaluate the electronic ground state of conjugated biradicals and to understand macroscopic magnetic and optical data with molecular level information.[16,10e,11a-c] To provide new insights into the correlation between their structures and properties, resonance Raman
15 experiments on **QDTP** and **QDTQ** were conducted at laser wavelengths of 785 and 633 nm respectively (Fig. 4), which are in resonance with their strongest electronic absorptions (*vide infra*) due to their singlet ground electronic states. We compare in Fig. 4 these spectra with those of the non-thiophenic homologues
20 with the same rylene core, **Per-CN** (λ_{exc} = 532 nm) and **QR-CN** (λ_{exc} = 785 nm).[11b]
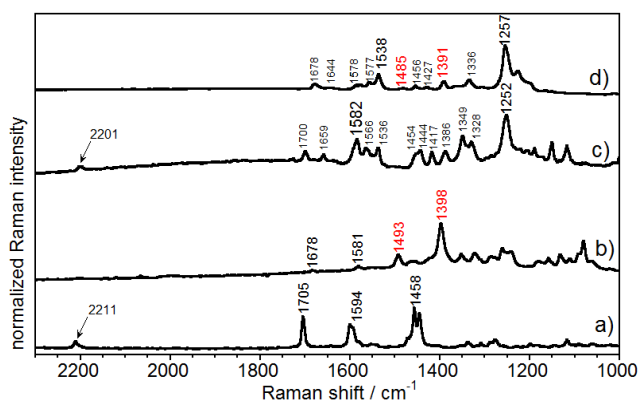

Fig. 4 Solid-state resonant Raman spectra of (a) **Per-CN** (λ_{exc} = 532 nm);
(b) **QDTP** (λ_{exc} = 785 nm), (c) **QR-CN** (λ_{exc} = 785 nm); and (d) **QDTQ**
25 (λ_{exc} = 633 nm).

The intense quinoidal bands of **Per-CN** at 1705, 1594, and 1458 cm^{-1} (Fig. 4a) became weaker and frequency down-shifted in **QDTP** at 1678 and 1581 and 1398 cm^{-1} respectively (Fig. 4b). In
30 particular, the ν (C=C) modes of the bonds attaching the dicyano groups to the thiophene cores change from 1458 cm^{-1} in full quinoidal **Per-CN** to 1398 cm^{-1} in **QDTP**, revealing the evolution from a C=C character towards a weaker C-C feature. The new band at 1493 cm^{-1} could be assigned to a C=C stretching mode of
35 the two thiophene rings as a similar strong Raman band with frequency at 1492 cm^{-1} was reported for aromatic dimethyl-bithiophene.[17] As a result, the most stable configuration of **QDTP** in the ground state can be ascribed to a singlet biradical promoted by the aromatization of the thiophene and NP moieties. As for the
40 ν(C≡N) bands around 2200 cm^{-1}, these are clearly observed as medium intensity Raman bands for closed-shell structures and experience a strong weakening, turning undetectable, in open-shell biradical species.[12b,16] This is the case of **Per-CN** and **QR-CN** with the well-resolved bands at 2211 and 2201 cm^{-1} (this
45 latter is borderline between closed-shell and open-shell) respectively, while no bands are observed within the same signal-to-noise ratio in **QDTP** and **QDTQ** revealing their biradical shapes. For the non-thiophenic derivatives, the Raman spectrum experienced a splitting and the appearance of new bands due to

50 the existence of new bonds on **Per-CN→QR-CN** (Fig. 4c). Several medium-weak bands around 1600 cm^{-1} in **QDTQ** could be attributed to modes of the central benzenoid moieties due to their aromatic shapes. The most intense Raman band was at 1257 cm^{-1} in **QDTQ** and was absent in **QDTP** and hence ascribable to
55 the tetrabenzo fused innermost group. Such intense Raman bands at the frequencies between 1250 and 1300 cm^{-1} have been reported in fused benzenoid polycyclic hydrocarbons.[18] The bands at 1485 and 1391 cm^{-1} in **QDTQ** can be related with the thiophenic bands at 1493 and 1398 cm^{-1} in **QDTP** bearing a
60 pseudo-aromatic character for the bithiophene moiety. Assuming the biradical character for **QDTP** and **QDTQ**, the larger separation between the two electrons in the radical centers of the latter benefits charge repulsion and produces a decrease of the singlet-triplet energy gap, in concordance with the SQUID
65 measurements. The singlet-triplet gaps in the non-thiophenic compounds are expected to be significantly larger due to their closed-shell ground state forms. Comparing **QDTP** and **QR-CN**, both with four pro-aromatic rings, the expression of biradical character in the former is related with the possibility of rotation
70 around the thiophene-rylene single bond in the biradical state which has been described as the driving force for the closed-shell rupture in the **nPer-CN** compounds. In line with this argument, Fig. S3 (ESI†) compares the 785 nm Raman spectra of **QDTP** in solid state and in dichloromethane (DCM) solution. Both spectra
75 display the 1493 cm^{-1} intra-ring thiophene aromatic band at the same value, while that at 1398 cm^{-1} in solid displaces to 1391 cm^{-1} in DCM revealing the distortion of the dicyanomethylene groups relative to the thiophenes as a result of the greater flexibility in the biradical state.
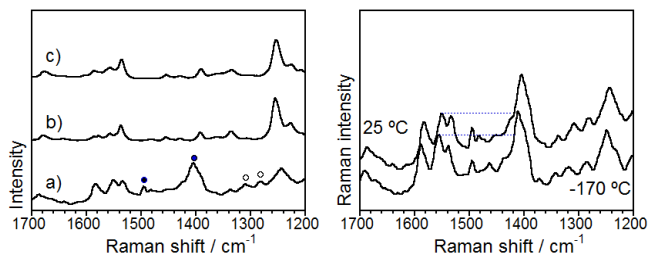

Fig. 5 (Left) Raman spectra of **QDTQ** at different excitation wavelengths:
a) 1064 nm, b) 633 nm, c) 532 nm. (Right) 1064 nm FT-Raman spectra of
QDTQ in solid state at different temperatures.

85 Given the small singlet-triplet energy gap, -0.16 kcal/mol in **QDTQ**, the first excited triplet might be significantly populated at room temperature by thermally activated intersystem crossing from the singlet ground electronic state. In contrast with the NMR data, the existence of triplets in ambient conditions allows
90 us to obtain their spectra by tuning the laser Raman excitation along the Vis-NIR spectrum. The Raman spectra of **QDTQ** obtained with the 532 and 1064 nm are shown in Figure 5 together with that of at 785 nm due to its ground state singlet. For **QDTQ**, the spectrum with 532 nm excitation was almost
95 identical to that at 633 nm corresponding to the singlet open-shell species (Fig. 5b,c). However, when excited with the 1064 nm laser, the spectrum is in resonance with the broad weak absorption extending from 1000 to 1300 nm which is a distinctive property of **QDTQ** regarding **QDTP** (see below). This 1064 nm
100 spectrum significantly changes and up to four new bands (marked with circles in Fig. 5) were in co-existence with those of the singlet. The most noticeable aspect was the strong band at 1404 cm^{-1} together with that at 1490 cm^{-1} which are due to the thiophene moieties. The enhancement of these two bands upon
105 resonance with this NIR band could indicate the preferred

reorganization of the electronic structure around the terminal thiophenes in the new species. This is in accordance with this species being the biradical triplet since the wavefunction of the molecular orbitals with the unpaired electrons in the triplet configuration must display zero overlap which is achieved by localizing them further apart in the thiophenes. Due to the small singlet-triplet gap, we could expect some changes in the relative intensity of the singlet and triplet as a function of the temperature. Fig. 5 also shows the spectra at room temperature together with that at -170 ºC. Upon cooling we observed that the intensity of the 1490/1404 cm^{-1} bands seemingly decrease regarding those at 1550 cm^{-1} or, in other words, the population of the triplet decreases regarding that of the singlet upon lowering the temperature. This is in agreement with: i) the singlet being the ground electronic state, and ii) the triplet being very close in energy to the singlet. Interestingly by exciting **QDTP** with the 532 nm laser we obtained a Raman spectrum with new features regarding that at 785 nm which are similar to those described for the triplet species of **QDTQ**. The detection of the triplet in the Raman experiment of **QDTP**, in despite of being 4.71 kcal/mol higher, is a consequence of the selective outstanding resonant intensity enhancement with the 532 nm excitation.
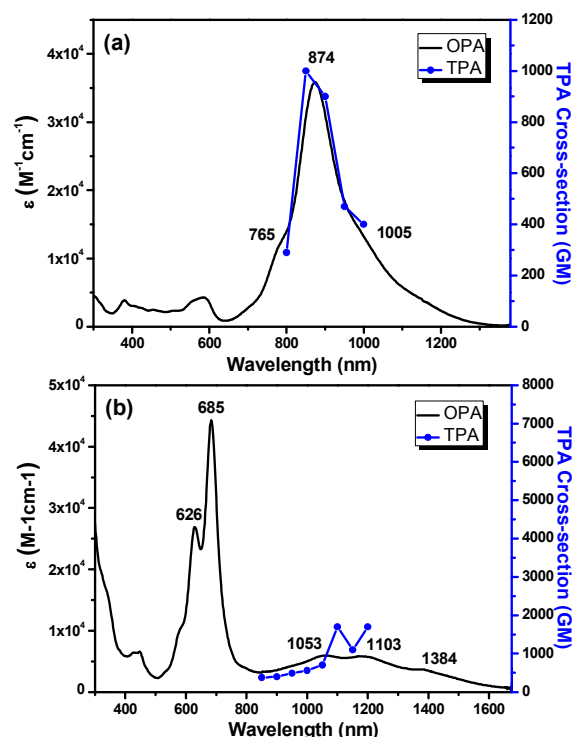
Optical properties

Fig. 6 OPA spectra (solid line and left vertical axis) and TPA spectra (blue symbols and right vertical axis) of (a) **QDTP** and (b) **QDTQ** recorded in DCM. TPA spectra are plotted at $\lambda_{ex}/2$.

Compounds **QDTP** and **QDTQ** exhibited very different one-photon absorption (OPA) spectra in DCM compared to their corresponding closed-shell counterparts **Per-CN** and **QR-CN**, respectively.[11a,11b] While the characteristic band at 626 nm together with a shoulder absorption at 579 nm was assigned to the typical quinoidal structure of **Per-CN**,[11a] one intense absorption band with maximum at 874 nm (log ε = 4.56), along with two unresolved shoulders at 765 and 1005 nm in the NIR region, was observed for **QDTP** (Fig. 6a). Remarkably, the longest

absorption tail reached the wavelength region of ~1400 nm, leading to a very small optical energy gap (0.94 eV). This big difference in the absorption band structure indicates that **QDTP** has a different ground-state electronic structure from the quinoidal **Per-CN**. **QR-CN** has a very similar band structure to **Per-CN**, with an intense absorption band at 880 nm and a shoulder at 798 nm.[11b] On passing to **QDTQ**, a band maximum at 685 nm (log ε = 4.34) with one shoulder at 626 nm was detected (Fig. 6b). This intense band experienced an obvious blue-shift in comparison with **QDTP** (approximately 189 nm), resulting in an absorption spectrum quite similar to that of the fused bis-*N*-annulated quaterrylene.[14] The most outstanding character is the existence of three overlapping bands in the infrared region with the absorption maxima at 1052, 1103 and 1384 nm, respectively. This spectral evolution is comparable to the band structure change from quinoidal **Per-CN** to the biradicals of higher series (**nPer-CN**s, n>2),[11a] and ascribable to the significant population of triplets in ambient conditions. An optical energy gap of 0.75 eV was determined for **QDTQ**. All these compounds showed no fluorescence due to their open-shell character.

Femtosecond transient absorption measurements were performed to explore the excited-state dynamics of **QDTP** and **QDTQ** (Fig. S4 in ESI†). Compound **QDTP** has a short singlet excited lifetime (τ = 1.6 ps), which is much shorter than that of **Per-CN** (τ = 17.2 ps).[11a] This fast decay indicates an acceleration of the non-radiative internal conversion arising from the shorter energy gap between the lowest excited state and the open-shell ground state. The decay profiles of **QDTQ** probed at 700 nm were fitted by a biexponential function with τ_1 = 0.4 ps and τ_2 = 11 ps (Fig. S4 in ESI†), which are also faster than that for **QR-CN** (τ = 24 ps). The short excited-state lifetimes of **QDTP** and **QDTQ** are in good agreement with their non-fluorescent properties. Two-photon absorption measurements were carried out for **QDTP** and **QDTQ** in DCM by the Z-scan technique in the NIR region from 1600 to 2400 nm where one-photon absorption contribution is negligible (Fig. 6 and Fig. S5 in ESI†, the TPA spectra are plotted at $\lambda_{ex}/2$ for comparison with the OPA spectrum). Large TPA cross sections ($\sigma^{(2)}$) were observed for both quinoidal chromophores, with $\sigma^{(2)}_{max}$ = 1000 GM at 1700 nm for **QDTP**, and $\sigma^{(2)}_{max}$ = 1700 GM at 2400 nm for **QDTQ**, which are comparable to the case of the biradicals **nPer-CN**s (n =2-5).[11a]

Electrochemical properties

Cyclic voltammetry and differential pulse voltammetry were used to investigate the electrochemical properties of **QDTP** and **QDTQ** (Fig. 7 and Fig. S6 in ESI†). In contrast to the **Per-CN** without obvious oxidative waves,[11a] **QDTP** demonstrated amphoteric redox behaviour with two chemically reversible oxidative processes with half-wave potential ($E_{1/2}^{ox}$) at -0.37 and 0.48 V, two chemically irreversible oxidation waves with $E_{1/2}^{ox}$ -0.03 and -0.69 V, and one reductive process with half-wave potential ($E_{1/2}^{red}$) at -1.37 V (*vs* Fc/Fc$^+$, Fc: ferrocene). The HOMO and LUMO energy levels were determined to be -4.40 and -3.57 eV, respectively, from the onset potentials of the first oxidation and reduction wave. On passing to **QDTQ**, five closely overlapping oxidative processes with $E_{1/2}^{ox}$ at -0.49, -0.21, -0.04, 0.37, 0.70 V were observed, together with four overlapping chemically irreversible reductive processes with $E_{1/2}^{red}$ at -1.50, -1.35, -1.09, -0.98 V. Accordingly, the HOMO and LUMO energy levels of **QDTQ** were estimated to be -4.23 and -3.86 eV, respectively. Rather low electrochemical energy gaps of 0.83 and 0.37 eV were determined for **QDTP** and **QDTQ**, respectively.
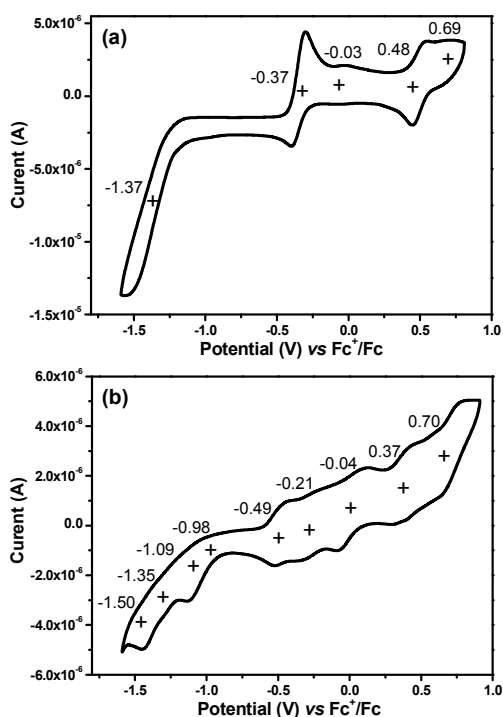
Fig.7 Cyclic voltammograms of (a) **QDTP** and (b) **QDTQ** in dry DCM with 0.1 M Bu$_4$NPF$_6$ as supporting electrolyte, Ag/AgCl as reference electrode, Au disk as working electrode, Pt wire as counter electrode, and scan rate at 50 and 20 mV/s, respectively.

Theoretical calculations

Broken-symmetry DFT (BS-UB3LYP/6-31G**) calculations were carried out to provide further understanding of the electronic structures and spectral findings in **QDTP** and **QDTQ**. The calculations revealed that both compounds have a singlet biradical ground state, agreeing with all experimental results. The singlet-triplet energy gap $\Delta E_{S\text{-}T}$ for **QDTP** and **QDTQ** was estimated to be -1.45 and -1.35 kcal/mol, respectively, and both show a relatively large deviation from the SQUID data, indicating the challenges to calculate a large open-shell system. However, the trend of increasing the conjugated length leading to a smaller singlet-triplet energy gap is in good agreement with observations for other polycyclic hydrocarbons.[19] The singlet biradical characters (y) of **QDTP** and **QDTQ** were estimated to be 0.81 and 0.93 by the CASSCF(2,2)/6-31G calculations.[20] The larger biradical character for **QDTQ** is consistent with the observed stronger ESR signal and larger magnetic susceptibility in SQUID experiments in comparison to **QDTP**. The molecular orbital profiles of **QDTP** and **QDTQ** exhibit a characteristic disjoint feature for the singly occupied molecular orbital (Fig. S7 and S8 in ESI†), which is a requisite to display small singlet-triplet gaps as seen in many singlet biradicals. The spin densities in these biradical species were distributed throughout the whole molecular framework and largely delocalized at the backbone of terminal malononitrile-substituted thiophene units (Fig. 8). This can further explain the more significant NMR signal broadening for the thiophene ring protons than those of NP units as shown in Fig. 2a.

Theoretical calculations also demonstrated an optimized geometry for the singlet biradical of **QDTP** with a moderate dihedral angle (34.3) between the thiophene and NP unit (Fig. S9 in ESI†) in agreement with the flexibility property described above. On passing to **QDTQ**, the dihedral angle of the singlet biradical becomes slightly smaller (33.0^o) (Fig. S9 in ESI†). This dihedral angles resulting from twisting the C=C bonds of the backbones play roles in generation of the biradical contribution. In comparison to the quinoidal **Per-CN**,[11a] these singlet biradicals showed longer bond lengths for the exo methylene bonds as the weakening of the C=C bonds was observed in the vibrational studies. It is also noteworthy that the C=C bonds between thiophene and rylene rings displayed a longer length in all states (closed-shell, singlet biradical and triplet) compared to the other double bonds along the π-extended quinodimethane chain (Fig. S9 in ESI†), indicating that the thiophene rings have a large aromatic character. On the basis of calculated nucleus independent chemical shift (NICS) values[21] (NICS(1) and NICS(1)$_{zz}$), both singlet biradicals of **QDTP** and **QDTQ** exhibited more benzenoid character for the NP moieties and aromatic characteristic for the thiophene units (Fig. S10 in ESI†), which are consistent with the Raman spectral findings. It also suggests that the recovery of aromaticity of the central rylene core and the side thiophene rings would be a driving force for the formation of singlet biradical in the ground state together with the conformational effect between the thiophenes and rylene.
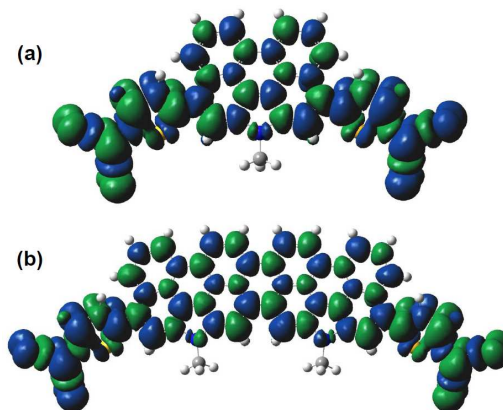

Fig. 8 Calculated (UB3LYP) spin density distribution of (a) **QDTP** and (b) **QDTQ**. Blue and green surfaces represent α and β spin densities, respectively. Isovalue is 0.002. The long branched *N*-alkyl chains are replaced by methyl groups during the calculations.

Time-dependent DFT calculations were conducted to predict the electronic absorption spectra of **QDTP** and **QDTQ** (Fig. S11 in ESI†). The characteristic low-lying excited states assigned by the admixing spin-associated (H, H → L, L) double excited electron configurations[22] were well identified in these biradical species and the lowest energy transitions (S$_0$→S$_1$) are predicted to be 1.02 eV (1200 nm, f = 0.0137) for **QDTP** and 0.78 eV (1574 nm, f = 0.0199) for **QDTQ**, respectively. Such smaller energy gaps are favourable to promote electrons from HOMO to LUMO and lead to an open-shell singlet biradical ground state. The other calculated transitions are close to the experimental observations (Tables S1 and S2 in ESI†).

Conclusions

In conclusion, two new soluble and stable tetracyano-dithienoperylene and dithienoquaterrylenequinodimethanes (**QDTP** and **QDTQ**) were successfully prepared and their electronic structures and geometries in the ground state were systematically investigated by various experimental methods and DFT calculations. Both of them have a singlet biradical ground state and such an evolution from closed-shell quinoids (**Per-CN/QR-CN**) to singlet biradicals (**QDTP/QDTQ**) can be

explained by the recovery of two additional aromatic thiophene rings in the biradical resonance forms together with the conformational flexibility around the thiophene-rylene connections. With extension of the conjugation length, the biradical character y increases from **QDTP** to **QDTQ** due to the decreased energy gap. Both chromophores showed very strong one-photon absorption and large two-photon absorption response in the near infrared region. Our studies demonstrated that the ground state of a closed-shell polycyclic hydrocarbon can be converted into a singlet biradical state by accurate tuning of its structure and aromaticity. In response to the change of ground state, the optical, electronic and magnetic properties of the open-shell species are significantly different from the closed-shell species. The obtained materials also possess potential applications for non-linear optics, ambipolar field effect transistors and organic spintronics and these studies are underway in our laboratories.

Notes and references

^{a} Department of Chemistry, National University of Singapore 3 Science Drive 3, 117543 (Singapore). Fax: 65-67791691; Tel: 65-65162677; E-mail: chmwuj@nus.edu.sg
^{b} Spectroscopy Laboratory for Functional π-Electronic Systems and Department of Chemistry, Yonsei University, Seoul 120-749, Korea; E-mail: dongho@yonsei.ac.kr
^{c} Department of Physical Chemistry, University of Malaga, Campus de Teatinos s/n, 229071 Malaga, Spain; E-mail: casado@uma.es (J. C.) and teodomiro@uma.es (J. T. L. N.)
^{d} Department of Materials Science & Engineering, National University of Singapore, 119260, Singapore; E-mail: msedingj@nus.edu.sg
^{e} Division of Chemistry & Biological Chemistry, School of Physical & Mathematical Sciences, Nanyang Technological University, 21 Nanyang Link, 637371, Singapore
*^{f} Institute of Materials Research and Engineering, A*STAR, 3 Research Link, Singapore, 117602*

Acknowledgements

†Electronic Supplementary Information (ESI) available: Synthetic procedures and characterization data of all other new compounds. Details for all physical characterizations and theoretical calculations. Additional spectroscopic and computational data. See DOI: 10.1039/b000000x/.

1. (*a*) C. Lambert, *Angew. Chem. Int. Ed.* 2011, **50**, 1756–1758. (*b*) Y. Morita, K. Suzuki, S. Sato and T. Takui, *Nat. Chem.* 2011, **3**, 197–204. (*c*) Z. Sun and J. Wu, *J. Mater. Chem.* 2012, **22**, 4151–4160. (*d*) Z. Sun, Q. Ye, C. Chi, C. and J. Wu, *Chem. Soc. Rev.* 2012, **41**, 7857−7889. (*e*) A. Shimizu, Y. Hirao, T. Kubo, M. Nakano, E. Botek and B. Champagne, *AIP Conf. Proc.* 2012, **1504**, 399–405. (*f*) Z. Sun, Z. Zeng and J. Wu, *Chem. Asian J.* 2013, **8**, 2894–2904. (*g*) M. Abe, *Chem. Rev.* 2013, **113**, 7011−7088.

2. K. Kamada, K. Ohta, T. Kubo, A. Shimizu, Y. Morita, K. Nakasuji, R. Kishi, S. Ohta, S.-I. Furukawa, H. Takahashi and M. Nakano, *Angew. Chem. Int. Ed*. 2007, **46**, 3544−3546.

3. (*a*) M. Chikamatsu, T. Mikami, J. Chisaka, Y. Yoshida, R. Azumi, and K. Yase, *Appl. Phys. Lett.* 2007, **91**, 043506. (*b*) D. T. Chase, A. G. Fix, S. J. Kang, B. D. Rose, C. D.Weber, Y. Zhong, L. N. Zakharov, M.

C. Lonergan, C. Nuckolls and M. M. Haley, *J. Am. Chem. Soc.* 2012, **134**, 10349−10352.

4. J. Lee, P. Jadhav, P. D. Reusswig, S. R. Yost, N. J. Thompson, D. N. Congreve, E. Hontz, T. Van Voorhis and M. A. Baldo, *Acc. Chem. Res.* 2013, **46**, 1300−1311.

5. Y. W. Son, M. L. Cohen and S. G. Louie, *Phys. Rev. Lett.* 2006, **97**, 216803.

6. Y. Morita, S. Nishida, T. Murata, M. Moriguchi, A. Ueda, M. Satoh, K. Arifuku, K. Sato and T. Takui, *Nat. Mater*. 2011, **10**, 947−951.

7. (*a*) A. Konishi, Y. Hirao, M. Nakano, A. Shimizu, E. Botek, B. Champagne, D. Shiomi, K. Sato, T. Takui, K. Matsumoto, H. Kurata and T. Kubo, *J. Am. Chem. Soc.* 2010, **132**, 11021–11023. (*b*) A. Konishi, Y. Hirao, K. Matsumoto, H. Kurata, R. Kishi, Y. Shigeta, M. Nakano, K. Tokunaga, K. Kamada and T. Kubo, *J. Am. Chem. Soc.* 2013, **135**, 1430−1437.

8. (*a*) D. T. Chase, B. D. Rose, S. P. McClintock, L. N. Zakharov and M. M. Haley, *Angew. Chem. Int. Ed.* 2011, **50**, 1127−1130. (*b*) A. Shimizu and Y. Tobe, *Angew. Chem. Int. Ed.* 2011, **50**, 6906–6910. (*c*) A. Shimizu, R. Kishi, M. Nakano, D. Shiomi, K. Sato, T. Takui, I. Hisaki, M. Miyata and Y. Tobe, *Angew. Chem. Int. Ed.* 2013, **52**, 6076–6079.

9. (*a*) K. Ohashi, T. Kubo, T. Masui, K. Yamamoto, K. Nakasuji, T. Takui, Y. Kai and I. Murata, *J. Am. Chem. Soc.* 1998, **120**, 2018–2027. (*b*) T. Kubo, M. Sakamoto, M. Akabane, Y. Fujiwara, K. Yamamoto, M. Akita, K. Inoue, T. Takui and K. Nakasuji, *Angew. Chem. Int. Ed.* 2004, **43**, 6474–6479. (*c*) T. Kubo, A. Shimizu, M. Sakamoto, M. Uruichi, K. Yakushi, M. Nakano, D. Shiomi, K. Sato, T. Takui, Y. Morita and K. Nakasuji, *Angew. Chem. Int. Ed.* 2005, **44**, 6564–6568. (*d*) A. Shimizu, M. Uruichi, K. Yakushi, H. Matsuzaki, H. Okamoto, M. Nakano, Y. Hirao, K. Matsumoto, H. Kurata and T. Kubo, *Angew. Chem. Int. Ed.* 2009, **48**, 5482–5486. (*e*) A. Shimizu, T. Kubo, M. Uruichi, K. Yakushi, M. Nakano, D. Shiomi, K. Sato, T. Takui, Y. Hirao, K. Matsumoto, H. Kurata, Y. Morita and K. Nakasuji, *J. Am. Chem. Soc.* 2010, **132**, 14421–14428. (*f*) A. Shimizu, Y. Hirao, K. Matsumoto, H. Kurata, T. Kubo, M. Uruichi and K. Yakushi, *Chem. Commun.* 2012, **48**, 5629–5631.

10. (*a*) R. Umeda, D. Hibi, K. Miki and Y. Tobe, *Org. Lett.* 2009, **11**, 4104−4106. (*b*) T. C. Wu, C. H. Chen, D. Hibi, A. Shimizu, Y. Tobe and Y. T. Wu, *Angew. Chem. Int. Ed.* 2010, **49**, 7059−7062. (*c*) Z. Sun, K.-W. Huang and J. Wu, *Org. Lett.* 2010, **12**, 4690–4693. (*d*) Z. Sun, K.-W. Huang and J. Wu, *J. Am. Chem. Soc.* 2011, **133**, 11896−11899. (*e*) Y. Li, W.-K. Heng, B. S. Lee, N. Aratani, J. L. Zafra, N. Bao, R. Lee, Y. M. Sung, Z. Sun, K.-W. Huang, R. D. Webster, J. T. López Navarrete, D. Kim, A. Osuka, J. Casado, J. Ding and J. Wu, *J. Am. Chem. Soc.* 2012, **134**, 14913−14922. (*f*) Z. Sun and J. Wu, *J. Org. Chem.* 2013, **78**, 9032–9040. (*g*) W. Zeng, M. Ishida, S. Lee, Y. M. Sung, Z. Zeng, Y. Ni, C. Chi, D.-H. Kim and J. Wu, *Chem. Eur. J.* 2013, **19**, 16814–16824. (*h*) L. Shan, Z.-X. Liang, X.-M. Xu, Q. Tang, and Q. Miao, *Chem. Sci.* 2013, **4**, 3294−3297. (*i*) Z. Sun, S. Lee, K. Park, X. Zhu, W. Zhang, B. Zheng, P. Hu, Z. Zeng, S. Das, Y. Li, C. Chi, R. Li, K.-W. Huang, J. Ding, D.-H. Kim and J. Wu, *J. Am. Chem. Soc.* 2013, **135**, 18229–18236.

11. (*a*) Z. Zeng, M. Ishida, J. L. Zafra, X. Zhu, Y. M. Sung, N. Bao, R. D. Webster, B. S. Lee, R.-W. Li, W. Zeng, Y. Li, C. Chi, J. T. López Navarrete, J. Ding, J. Casado, D.-H. Kim and J. Wu, *J. Am. Chem. Soc.* 2013, **135**, 6363−6371. (*b*) Z. Zeng, S. Lee, J. L. Zafra, M. Ishida, X. Zhu, Z. Sun, Y. Ni, R. D. Webster, R.-W. Li, J. T. López Navarrete, C. Chi, J. Ding, J. Casado, D.-H. Kim and J. Wu, *J. Angew. Chem. Int. Ed.* 2013, **52**, 8561−8565. (*c*) Z. Zeng, Y. M. Sung, N. Bao, D. Tan, R. Lee, J. L. Zafra, B. S. Lee, M. Ishida, J. Ding, J. T. López Navarrete, Y. Li, W. Zeng, D.-H. Kim, K.-W. Huang, R. D. Webster, J. Casado and J. Wu, *J. Am. Chem. Soc.* 2012, **134**, 14513−14525. (*d*) L. K. Montgomery, J. C. Huffman, E. A. Jurczak and M. P. Grendze, *J. Am. Chem. Soc.* 1986, **108**, 6004–6011.

12. (*a*) T. Takahashi, K. I. Matsuoka, K. Takimiya, T. Otsubo and Y. Aso, *J. Am. Chem. Soc.* 2005, **127**, 8928–8929. (*b*) R. P. Ortiz, J. Casado, S. R. Gonzalez, V. Hernandez, V.; J. Casado, V. Hernandez, J. T. López Navarrete, P. M. Viruela, E. Orti, K. Takimiya and T. Otsubo, *Angew. Chem. Int. Ed*. 2007, **46**, 9057–9061.

13. M. Uno, K. Seto, M. Masuda, W. Ueda and S. Takahashi, *Tetrahedron Lett.* 1985, **26**, 1553–1556.

14. (*a*) Y. Li and Z. Wang, Z. *Org. Lett.* 2009, **11**, 1385–1387. (*b*) C. Jiao, K. Zhang, C. Chi and J. Wu, *Org. Lett.* 2009, **11**, 4508–4511. (*c*) C. Jiao, K.-W. Huang, Z. Guan, Q.-H. Xu and J. Wu, *Org. Lett.* 2010, **12**, 4046−4049. (*d*) Y. Li, J. Gao, S. I. Motta, F. Negri and Z. Wang, *J. Am. Chem. Soc.* 2010, **132**, 4208–4213.

15. B. Bleaney and K. D. Bowers, *Proc. R. Soc. London Ser. A.* 1952, **214**, 451−465.

16. (*a*) J. Casado, S. Patchkovskii, M. Z. Zgierski, L. Hermosilla, C. Sieiro, M. Moreno Oliva and J. T. López Navarrete, *Angew. Chem. Int. Ed.* 2008*, 47,* 1443–1446. (*b*) S. R. González, Y. Ie, Y. Aso, J. T. López Navarrete and J. Casado, *J. Am. Chem. Soc.* 2011, **133**, 16350−16353.

17. J. Casado, R. G. Hicks, V. Hernández, D. J. T. Myles, M. C. R. Delgado and J. T. López Navarretea, *J. Chem. Phys.* 2003, **118**, 1912-1920.

18. J. Wu, L. Gherghel, M. D. Watson, J. Li, Z. Wang, C. D. Simpson, U. Kolb and K. Müllen, *Macromolecules.* 2003, **36***,* 7082-7089.

19. (*a*) S. D. Motta, F. Negri, D. Fazzi, C. Castiglioni and E. V. Canesi, *J. Phys. Chem. Lett.* 2010, **1**, 3334–3339. (*b*) K. Kamada, K. Ohta, A. Shimizu, T. Kubo, R. Kishi, H. Takahashi, E. Botek, B. Champagne and M. Nakano, *J. Phys. Chem. Lett.* 2010, **1**, 937–940.

20. D. Döýhnert and J. Koutecký, *J. Am. Chem. Soc.* 1980, **102**, 1789−1796.

21. Z. F. Chen, C. S. Wannere, C. Corminboeuf, R. Puchta and P. V. Schleyer, *Chem. Rev.* 2005, **105**, 3842−3888.

22. S. D. Motta, F. Negri, D. Fazzi, C. Castiglioni and E. V. Canesi, *J. Phys. Chem. Lett.* 2010, **1**, 3334–3339.

Chemical Science Accepted Manuscript